Redefining cholesterol's role in the mechanism of the cholesterol-dependent cytolysins

Kara S. Giddings*, Arthur E. Johnson†‡§, and Rodney K. Tweten*¶

*Department of Microbiology and Immunology, University of Oklahoma Health Sciences Center, Oklahoma City, OK 73104; †Department of Medical Biochemistry and Genetics, Texas A&M University System Health Science Center, College Station, TX 77843-1114; and Departments of ‡Chemistry and §Biochemistry and Biophysics, Texas A&M University, College Station, TX 77843

Edited by John J. Mekalanos, Harvard Medical School, Boston, MA, and approved August 6, 2003 (received for review June 9, 2003)

The cholesterol-dependent cytolysins (CDCs) constitute a large family of pore-forming toxins that function exclusively on cholesterol-containing membranes. A detailed analysis of the various stages in the cytolytic mechanism of three members of the CDC family revealed that significant depletion of cholesterol from the erythrocyte membrane stalls these toxins in the prepore complex. Therefore, the depletion of membrane cholesterol prevents the insertion of the transmembrane β-barrel and pore formation. These unprecedented findings provide a paradigm for the involvement of cholesterol in the CDC cytolytic mechanism and that of other pore-forming toxins whose activity is enhanced by the presence of membrane cholesterol.

The cholesterol-dependent cytolysins (CDCs) contribute to the pathogenesis of a large number of Gram-positive bacterial pathogens and belong to a superfamily of structurally unrelated pore-forming toxins recently termed the β-pore-forming toxins (β-PFTs) (1). The CDC cytolytic mechanism requires the presence of membrane cholesterol, and for over two decades cholesterol has been considered to be the receptor for the CDCs (reviewed in refs. 2 and 3) based on several lines of evidence including one that CDCs are not cytolytically active on cholesterol-deficient membranes and another that the depletion of membrane cholesterol reduces the extent of membrane binding to various eukaryotic cell types (4). Many studies, primarily performed with perfringolysin O (PFO), have shown that membrane binding is sensitive to the loss of cholesterol (4–11) and that derivatives of PFO have been used as probes for membrane cholesterol (12–15).

However, studies on other members of the CDC family suggest that the loss of membrane binding may not account for the extreme sensitivity of these toxins to membrane cholesterol levels. The CDC from *Streptococcus intermedius*, intermedilysin (ILY), exhibits an exquisite specificity for human cells (16), suggesting that cholesterol cannot be responsible for membrane recognition by ILY, yet its mechanism still seems sensitive to cholesterol (16). Also, Jacobs *et al.* (17) have shown that the addition of exogenous cholesterol inhibited the activity of the CDC listeriolysin O (LLO) but did not prevent its binding to the membrane. Hence, the mechanism by which cholesterol affects the cytolytic activity of the CDCs remains ambiguous even though the dependence of the CDC cytolytic mechanism on the presence of membrane cholesterol is the defining property of these toxins.

These inconsistencies in cholesterol's role in the CDC mechanism prompted us to make a detailed examination of the effects of cholesterol on each stage of the cytolytic mechanism of three different CDCs: PFO, streptolysin O (SLO), and ILY. In stark contrast to the dogma that cholesterol sensitivity of the CDCs resides in the receptor-binding event, we have found that the depletion of membrane cholesterol of human erythrocytes prevents insertion of the transmembrane β-barrel and traps the CDCs in the prepore complex.

Materials and Methods

Bacterial Strains, Plasmids, and Chemicals. The gene for PFO^{C459A} (cysteine-less derivative of PFO) was cloned into pTrcHisA (Invitrogen) and expressed as described (18). DNA sequencing was carried out by the DNA sequencing Core Facility at the Oklahoma Medical Research Foundation (Oklahoma City, OK). All chemicals and enzymes were obtained from Sigma except where noted. Cholesterol was obtained from Avanti Polar Lipids. All fluorescent probes were obtained from Molecular Probes.

Generation and Purification of PFO, SLO, ILY, and Their Derivatives. Amino acid substitutions in the various genes for PFO, SLO, and ILY were generated either by PCR overlap mutagenesis (19) or PCR QuikChange mutagenesis (Stratagene) by using the gene for a cysteine-less derivative of PFO (18), or SLO (E.M.H. and R.K.T., unpublished results). The gene for ILY was cloned from the Gram-positive bacteria *S. intermedius* by using the following pTrcHisA vector primers for ILY: *Bam*HI-GGGCCGGATCCGAAACACCTACCAAACCAAAAGC and *Eco*RI-GGGCCCTTAAGTTAATCAGTGTTATCTTTCACAAC. The gene for SLO was cloned from *Streptococcus pyogenes* by using the following pTrcHisA vector primers for SLO: *Bam*HI-CCGCGGATCCGCTCCCAAAGAAATGCCACTA and *Eco*RI-CGACGAATTCCTACTTATAAGTAATCGAACCATA. Expression and purification of all three proteins and their derivatives used in this study were carried out as before for PFO (18).

Hemolytic Activity. The hemolytic activity of each toxin on native and cholesterol-depleted human erythrocytes (hRBCs) was determined as previously described by Shepard *et al.* (18). The HD_{50} is defined as the concentration of toxin required to lyse 50% of the hRBCs in 50 μl of PBS containing ≈2.5×10^6 hRBCs.

Membrane Cholesterol Depletion and Restoration. Cholesterol extraction with methyl-β-cyclodextrin was done as described (20) with modifications. Freshly drawn hRBCs were pelleted by centrifugation at 1,500 × *g* for 8 min and washed three times with PBS [10 mM Na_2HPO_4 (pH 7.5) containing 147 mM NaCl and 3 mM KCl]. Cholesterol depletion was accomplished by suspending the hRBCs in PBS containing 3.5 mM methyl-β-cyclodextrin (MβCD) [final hematocrit of 5% (vol/vol)] for 120 min at 37°C. The hRBCs were washed three times with PBS to remove the MβCD and associated cholesterol. Half of the cells were used for flow cytometry, and the other half were used to determine cholesterol content (Cholesterol 20 assay, Sigma). The relative depletion of the MβCD was equal to the concen-

This paper was submitted directly (Track II) to the PNAS office.

Abbreviations: hRBC, human RBC; CDC, cholesterol-dependent cytolysins; PFO, perfringolysin O; SLO, streptolysin O; ILY, intermedilysin; MβCD, methyl-β-cyclodextrin; FRET, fluorescence resonance energy transfer; SDS/AGE, SDS/agarose gel electrophoresis; TMH, transmembrane β-hairpin; NBD, *N,N′*-dimethyl-*N*-(iodoacetyl)-*N′*-(7-nitrobenz-2-oxa-1,3-diazolyl)ethylene-diamine.

¶To whom correspondence should be addressed at: Department of Microbiology and Immunology, BMSB-1053, University of Oklahoma Health Sciences Center, Oklahoma City, OK 73104. E-mail: rod-tweten@ouhsc.edu.

tration of cholesterol in the native hRBCs/concentration of cholesterol in the native hRBCs. Approximately 90% of the total hRBC cholesterol was removed primarily because erythrocyte cholesterol is almost entirely associated with the plasma membrane of erythrocytes (20).

To restore cholesterol to the cholesterol-depleted hRBCs, the cells were centrifuged and suspended in a buffer containing cholesterol/MβCD prepared as described (21) except that cholesterol was added to make a final concentration of 4 mM in 10 ml of buffer A (140 mM NaCl/5 mM KCl/5 mM KH_2PO_4/1 mM $MgSO_4$/10 mM Hepes/5 mM glucose, pH 6.5) containing 5 mM MβCD. Depleted cells were suspended in the cholesterol-loaded MβCD buffer A to a final hematocrit of 5% (vol/vol) and incubated for 120 min at 37°C. The cells were then washed three times in PBS to remove any residual cholesterol–MβCD complex.

Modification of Proteins with Fluorescent Probes. The labeling of the PFO, ILY, and SLO derivatives was carried out as described for PFO (22) except that Alexa Fluor 488 C_5 maleimide or iodoacetamido-*N*,*N*′-dimethyl-*N*-(iodoacetyl)-*N*′-(7-nitrobenz-2-oxa-1,3-diazolyl)ethylene-diamine (NBD; Molecular Probes) was used to label the proteins. The dye-labeled protein samples were made 10% (vol/vol) in glycerol, quick-frozen in liquid nitrogen, and stored at −80°C.

Membrane Binding by Flow Cytometry. Binding of each toxin labeled with Alexa Fluor 488 to hRBCs was determined as follows. To minimize any effects from self-quenching of the fluorescent probes, equimolar amounts of dye-labeled and unlabeled toxin were used in each experiment to sufficiently separate the dye molecules in the oligomer (23). Approximately 4.5 pmol each of dye-labeled toxin and unlabeled toxin were equilibrated at 4°C with 50 μl of PBS containing 0.1% BSA. Freshly drawn (washed three times in buffer A) hRBCs (1.5×10^6; 25–30 μl) were added to the toxin mixture at 4°C and allowed to incubate for 30 min. The hRBCs with bound toxin were then diluted to a final volume of 400 μl in PBS at 4°C and analyzed by using a FACSCalibur flow cytometer (University of Oklahoma Health Sciences Center) and FLOWJO software (Tree Star, San Carlos, CA). The emission wavelength was set to 530 nm, and the excitation was set at 488 nm with a bandpass of 30 nm.

Fluorescence Resonance Energy Transfer (FRET) by Flow Cytometry. FRET-based flow cytometry experiments were similar to those performed for binding experiments, with the following changes. Equimolar amounts (4.5 pmol each) of donor-labeled toxin (D) (Alexa Fluor 488-labeled toxin) and either unlabeled toxin (U) or acceptor-labeled toxin (A) (tetramethylrhodamine-labeled toxin) were added to native or cholesterol-depleted hRBCs. The mixtures were then analyzed by flow cytometry as in the binding experiments. Changes in the donor fluorescence due to FRET were determined by comparing donor fluorescence in the presence of acceptor-labeled toxin (D + A) to that when acceptor was replaced with unlabeled toxin (D + U). The net change in intensity due to FRET was determine by comparison of D + U and D + A. The emission and excitation settings were as described above for the binding analysis.

Membrane Insertion Measurements by Flow Cytometry. The change in fluorescence intensity of the NBD fluorophore attached to PFO^{A215C} when buried in the bilayer during insertion of transmembrane β-hairpin 1 (TMH1) has been described (24). For SLO and ILY, we placed the NBD-probe at the analogous residues, SLO^{S287C} and ILY^{H242C}. Samples containing 9 pmol of NBD-labeled PFO, SLO, or ILY were incubated with 1.5×10^6 hRBCs at 4°C for 30 min to allow toxin to bind and oligomerize. These samples were then analyzed by flow cytometry. To stimulate the insertion of the transmembrane β-hairpins, the sample was shifted to 37°C for 10 min (24) and was analyzed again by flow cytometry. The emission and excitation wavelengths and the bandpass setting for the flow cytometer were the same as for the binding analysis.

To confirm that NBD probe was inserted into the membrane, the toxin-treated native and cholesterol-depleted erythrocyte samples from the above experiments were equilibrated with 50 μg of a 1:1 mixture of 5- and 16-doxyl-stearic acid (Sigma) in MeOH by gentle vortexing at room temperature. The samples were then analyzed by flow cytometry as described above.

SDS/Agarose Gel Electrophoresis (SDS/AGE) and Immunoblot Analyses. Denaturing agarose gel electrophoresis was carried out as established by Shepard *et al.* (18) except that each toxin (9 pmol) was incubated with 1.5×10^6 native or cholesterol-depleted hRBCs for 30 min at 37°C.

hRBC Ghost Membrane Preparation. hRBC ghost membranes were prepared as described (23) with some modifications. After hypotonic lysis of the hRBCs, cytoplasmic constituents were separated from the membranes by dialysis with 2 liters of the lysis buffer [5 mM sodium phosphate (monobasic), pH 7.5, containing 1 mM EDTA] by recirculation through a Filtron tangential flow Centramate unit (Pall) equipped with 100-kDa cutoff membranes at 20 psi (1 psi = 6.89 kPa). Membrane protein concentration was determined by the method of Bradford (25) by using BSA as the protein standard.

Steady-State Fluorescence Spectroscopy. Fluorescence intensity measurements were performed by using an SLM-8100 photon-counting spectrofluorimeter equipped with a dual grating excitation monochromator, a single emission monochromator with a Peltier-cooled photomultiplier tube, and a 450-watt xenon lamp as described (18). An excitation wavelength of 470 nm was used for NBD, and the emission intensity was measured from 500 to 600 nm; the bandpass was 2 nm for all NBD measurements. Emission scans of each sample were carried out at a resolution of 1 nm with an integration time of 1 s. In a typical experiment, 17 pmol of toxin was incubated alone or in the presence of native, cholesterol-depleted, or cholesterol-replete erythrocyte ghost membranes (equivalent to 10 μg of membrane protein) for 30 min at 37°C. Data obtained from control samples with or without membranes containing unlabeled toxin were subtracted from the fluorescence spectra to determine the net fluorescence intensity.

Fluorescence quenching experiments were performed in the same manner except the membranes were equilibrated with a 1:1 (wt/wt) mixture of 5- and 16-doxyl-stearic acid quenchers to introduce a nitroxide into the bilayer core. Each probe was dissolved in MeOH to a final concentration of 50 mg/ml. Erythrocyte ghost membranes were equilibrated with 200 μg of probe per 1 mg of membrane protein. The doxyl-stearic acid was equilibrated with the membranes for 10 min at room temperature with gentle rocking. Unincorporated probe was removed by washing the membranes three times in buffer A.

Results

Depletion of Membrane Cholesterol Abolishes CDC-Dependent Erythrocyte Lysis. The effect of cholesterol depletion on the sensitivity of hRBCs to lysis by PFO, SLO, or ILY was initially examined to confirm that the cytolytic mechanism of all three toxins was indeed sensitive to the loss of membrane cholesterol. The hemolytic dose for 50% lysis (HD_{50}, see *Materials and Methods*) was determined for each toxin by using native hRBCs and hRBCs depleted of ≈90% of their membrane cholesterol (Table 1) with the cholesterol-sequestering agent MβCD (20, 26).

The loss of membrane cholesterol resulted in a >11,000-fold

Table 1. Hemolytic activity on native, cholesterol-depleted, and cholesterol-replete hRBCs

CDC	HD_{50}, fmol			
	Native hRBCs	Cholesterol-depleted hRBCs	Cholesterol-replete hRBCs	Fold change native/Chol$^-$
PFO	9.8	>86,000	9.2	>11,000
SLO	20.0	>89,000	26.5	>4,400
ILY	5.6	>17,000	6.6	>3,000

The HD_{50} (hemolytic dose for 50% lysis; see *Materials and Methods*) of PFO, SLO, and ILY was compared among native hRBCs, hRBCs depleted of 90% of the membrane cholesterol, and cholesterol-depleted hRBCs to which cholesterol was restored by using cholesterol-loaded MβCD.

increase in the HD_{50} of PFO, a >4,400-fold increase in the HD_{50} for SLO, and a >3,000-fold increase in the HD_{50} for ILY (Table 1). In all cases, the hemolytic activity of each toxin was reduced to <0.1% of its original activity, confirming that all three CDCs were highly sensitive to the loss of membrane cholesterol. Furthermore, the HD_{50} for all toxins was fully recovered when cholesterol was restored to the erythrocyte membrane by incubating the same depleted hRBCs with cholesterol-saturated MβCD inclusion complexes (Table 1) before carrying out the hemolytic assay. The latter experiment confirmed that only the loss of cholesterol was responsible for the loss of activity and not another component of the membrane that may have been coincidentally extracted by the MβCD treatment.

Cellular Binding of PFO, SLO, and ILY to Cholesterol-Depleted hRBCs. Membrane binding of PFO, SLO, and ILY to native and cholesterol-depleted hRBCs (as prepared above) was determined by using fluorescent-labeled toxins and flow cytometry. All toxins were extrinsically labeled at approximately a 1:1 molar ratio with the fluorescent dye at a unique cysteine in each toxin (see *Materials and Methods*). Because the toxin was directly labeled at an equimolar ratio with the fluorescent dye, any fluorescence-detected changes in binding determined by flow cytometry will accurately reflect the number of bound toxin molecules. Using extrinsically labeled toxin minimizes the inherent inaccuracies associated with indirect assays by using, for example, fluorescently tagged antibody to detect the toxin, where the number of dyes per antibody can vary and where the ratio of antibody to toxin could vary depending on the structural state of the toxin.

As can be seen in Fig. 1, cholesterol extraction decreased PFO binding by ≈10-fold. Surprisingly, SLO and ILY binding to the hRBCs was largely unaffected by the depletion of membrane cholesterol (Fig. 1), whereas their hemolytic activity on the same hRBCs was reduced >99.9% (Table 1). Furthermore, the

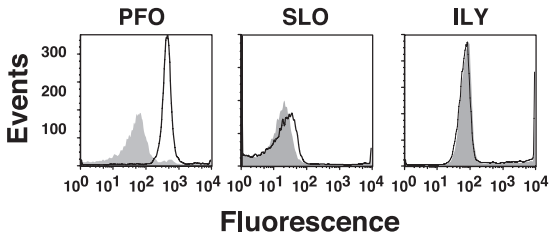

Fig. 1. Binding to native hRBCs and cholesterol-depleted hRBCs. Binding of fluorescently labeled derivatives of PFO^{A215C}, SLO^{G128C}, and ILY^{S57C} to hRBCs was determined by flow cytometry. The fluorescent-labeled toxin (4.5 pmol) was mixed with an equimolar amount of unmodified toxin, incubated with 1.5×10^6 hRBCs at 4°C for 30 min, and then analyzed by flow cytometry. We counted 10^4 cells per sample. Toxin binding to native (outlined peak) and cholesterol-depleted (shaded peak) hRBCs is shown for all three toxins.

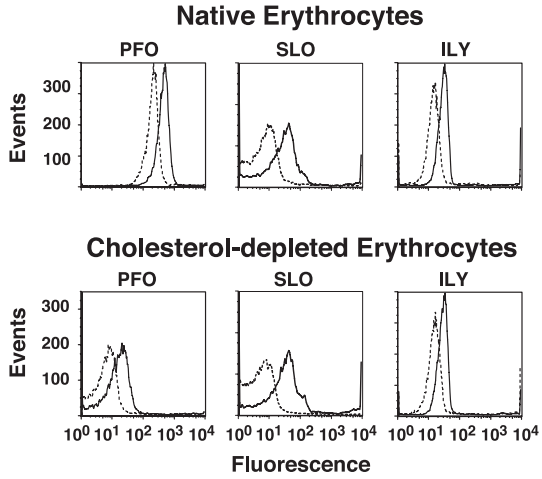

Fig. 2. Oligomerization measured by FRET and flow cytometry. Equimolar amounts (4.5 pmol each) of donor-labeled toxin (Alexa Fluor-labeled toxin) and either unlabeled (D + U, solid line) or acceptor-labeled (D + A, dashed line) toxin (tetramethylrhodamine-labeled toxin) were incubated with 1.5×10^6 hRBCs at 4°C for 30 min and then analyzed by flow cytometry. 10^4 cells per sample were counted. The fluorescence intensity of the donor fluorophore is shown for all three toxins on native and cholesterol-depleted hRBCs in the presence of unlabeled (D + U) or acceptor-labeled toxin (D + A). FRET between donor- and acceptor-labeled toxin is observed as a decrease in the fluorescence of the donor when the unlabeled toxin is replaced with acceptor-labeled toxin (compare D + U and D + A).

>11,000-fold decrease in hemolytic activity of PFO did not correlate with the 10-fold decrease in binding. These observations suggested that another stage of the mechanism was sensitive to the loss of cholesterol.

Oligomer Formation by the CDCs on Native and Cholesterol-Depleted Erythrocytes. After membrane binding, the CDC monomers diffuse laterally on the membrane and interact with one another to form a large oligomerized prepore complex (22, 24). When the prepore is formed, the complex inserts its transmembrane β-sheet (22, 24, 27, 28). The capacity of bound PFO, SLO, and ILY to oligomerize into a prepore complex was examined on native and cholesterol-depleted hRBCs by FRET by using flow cytometry, and these results were confirmed by the direct examination of oligomer formation by SDS/AGE.

FRET between donor- and acceptor-labeled toxin molecules was determined by flow cytometry to examine the oligomerization of each toxin under conditions similar to the binding experiments. Equimolar amounts of donor-labeled toxin (Alexa Fluor-labeled toxin) and either unlabeled toxin (D + U) or acceptor-labeled toxin (D + A) were used. As can be seen in Fig. 2, the magnitude of donor intensity decreased when the unlabeled toxin was replaced with acceptor-labeled toxin. Furthermore, the magnitude of the change was similar on both native and cholesterol-depleted hRBCs for all three toxins. As expected, the peaks of fluorescence intensity of the PFO in the absence and presence of the acceptor-labeled PFO were both shifted to the left (decreased total fluorescence) on the cholesterol-depleted membranes because PFO binds less efficiently to cholesterol-depleted membranes (Fig. 1). The magnitude of the change in the fluorescence intensity of the donor due to FRET in the presence of acceptor-labeled PFO was similar on both the native and cholesterol-depleted membranes, suggesting that, although less PFO was bound, the bound PFO oligomerized to the same extent as that on the native hRBCs.

We confirmed these observations by examining the formation of oligomers on the hRBCs by SDS/AGE (22, 24, 27). Again,

BIOCHEMISTRY

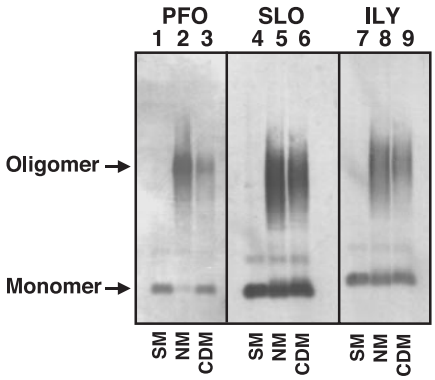

Fig. 3. Oligomer formation on native and cholesterol-depleted hRBCs determined by SDS/AGE. The formation of oligomers of PFO, SLO, and ILY was determined by SDS-agarose electrophoresis. Each toxin (9 pmol) was incubated alone (SM, soluble monomer), or with 1.5×10^6 native (NM) or cholesterol-depleted (CDM) hRBCs for 30 min at 37°C. The samples were solubilized with SDS sample buffer, the monomer and oligomeric complexes were resolved on a 1.5% SDS/AGE gel and immunoblotted, and the toxin was detected with specific antibody. Shown are the autoradiograms of the monomer and oligomer bands recognized by the antibody. Immunoblot analysis of untreated erythrocytes did not reveal any cross-reactive proteins (data not shown).

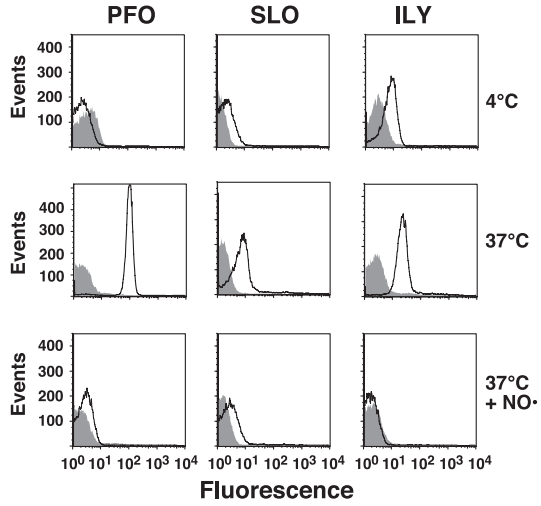

Fig. 4. Membrane insertion into native and cholesterol-depleted hRBCs. PFO, SLO, or ILY (9 pmol each), each labeled with NBD in a membrane-facing residue in TMH1, were incubated with 1.5×10^6 hRBCs at 4°C for 30 min and analyzed by flow cytometry. At 4°C, binding and oligomerization proceed, but insertion of the TMHs is significantly inhibited (24). Each sample was then shifted to 37°C for an additional 10 min to allow insertion of the TMHs and then was analyzed again by flow cytometry for changes in NBD emission. To confirm that the increase in NBD intensity seen with native hRBCs was due to TMH membrane insertion, the same sample was equilibrated with the collisional quencher doxyl-stearic acid (37°C + NO·), which places a nitroxide in the bilayer of the erythrocytes. The sample was then analyzed for a third time by flow cytometry. We counted 10^4 cells per sample in all experiments. Changes in the NBD intensity are shown for the toxins incubated with native (outlined peak) and cholesterol-depleted (shaded peak) hRBCs under each condition.

hRBCs were treated with each toxin under conditions similar to those used in the cellular binding assays and the FRET experiments above. The resultant toxin oligomers were then resolved from monomer by SDS/AGE (24). The prepore and pore oligomers of the CDCs are resistant to dissociation by SDS at 37°C although the prepore complex is slightly less resistant to dissociation than the pore complex (22). After separation of the proteins by SDS/AGE, the proteins were transferred to nitrocellulose paper, and the monomer and oligomer bands were identified by using toxin-specific antibodies. In all cases, significant oligomer is present on both native and cholesterol-depleted hRBCs (Fig. 3). However, because ≈10-fold less PFO binds to the cholesterol-depleted hRBCs, we see an overall reduction of the oligomer band. For both SLO and ILY, slightly less oligomer is present on the cholesterol-depleted membranes. However, the slight difference in the intensity of the oligomer bands cannot account for the loss of >99.9 of the hemolytic activity. Hence, cholesterol levels did not significantly affect the oligomerization of the toxins after they were bound to the membrane.

Membrane Insertion of the CDC Transmembrane β-Barrel Requires the Presence of Membrane Cholesterol. The final step in the CDC cytolytic mechanism is the conversion of the prepore complex to the pore complex by the insertion of the TMHs (18, 22, 24, 27, 29, 30). The insertion of the TMHs of all three toxins was detected by the increase in the fluorescence intensity of the fluorescent NBD probe when attached to a cysteine that has been substituted for a membrane-facing residue within TMH1 of PFO, SLO, or ILY (18, 22, 27, 29, 30). The location of the probe within the membrane is confirmed by collisional quenching by a nitroxide-labeled lipid (doxyl-stearic acid) that is introduced into the bilayer (18, 29).

The insertion of the transmembrane domains for each toxin was first examined on native and cholesterol-depleted hRBCs by flow cytometry under conditions identical to those used in the binding and FRET assays. However, in this case, we used the NBD-labeled derivatives of PFO, SLO, and ILY instead of the Alexa Fluor dye to detect insertion by an increase in fluorescence intensity as NBD moves into the hydrophobic environment of the bilayer. Initially, the fluorescence intensity of the NBD was determined after the toxins had formed the prepore complex on hRBCs by maintaining the temperature at 4°C (24, 28). As can be seen in all cases, the fluorescence intensity of the peaks was much lower than that observed for Alexa Fluor-labeled toxin because of the low quantum yield of NBD in a polar environment (Fig. 4). The sample was then warmed to 37°C to trigger the insertion of the transmembrane domains of the prepore to form the pore complex. For all toxins there is a significant increase in the fluorescence intensity of each sample indicating that the NBD had moved into a nonpolar environment (Fig. 4), presumably the membrane bilayer.

The location of the NBD in the bilayer was confirmed by incubating the same sample with 5- and 16-doxyl-stearic acid. The stearic acid quickly partitions into the membrane, thereby placing the nitroxide within the bilayer core (31). If the insertion of the toxin transmembrane domain places the NBD probe within the membrane, then the increase in the NBD fluorescence intensity observed as a result of insertion of the TMH into the bilayer should be significantly quenched by the presence of the membrane-restricted nitroxide. In all cases the fluorescence intensity of each inserted toxin is quenched to or below the fluorescence intensity of the uninserted prepore at 4°C, showing that each probe had inserted into the membrane (Fig. 4).

In contrast, there is little or no insertion of the toxins on the cholesterol-depleted hRBCs because little or no change in the fluorescence intensity of the NBD was observed when these samples were shifted to 37°C (Fig. 4). Therefore, it seems that the insertion of the TMHs into the membranes of the cholesterol-depleted cells did not occur. As expected, no decrease in the already low fluorescence intensity observed in these samples occurred when the hRBCs were equilibrated with the doxyl-stearic acid because there is no insertion of the TMHs. These observations strongly correlate with the loss of cytolytic activity on depletion of membrane cholesterol and suggest that the

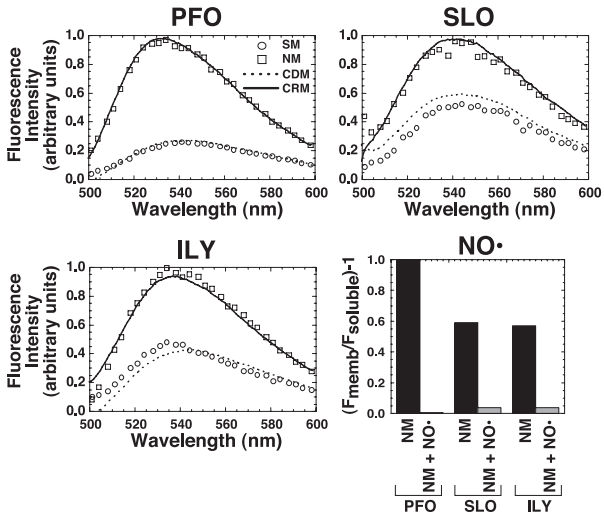

Fig. 5. Membrane insertion into native hRBC, cholesterol-depleted, or cholesterol-replete membranes. The fluorescence intensity of the same NBD-labeled toxin used for the experiments in Fig. 4 was determined when they were incubated alone (SM, soluble monomer) or with erythrocyte ghost native membranes (NM), cholesterol-depleted membranes (CDM), or cholesterol-replete membranes (CRP). The samples were incubated for 30 min at 37°C, and the emission intensities of the NBD for each sample were measured between 500 and 600 nm. To confirm that the NBD-labeled residues of SLO and ILY were membrane facing, the same experiment was repeated for each labeled toxin in the absence and presence of the membrane collisional quencher doxyl-stearic acid (graph labeled NO·). Only the net emission intensity of the NBD at 540 nm [$(F_{memb}/F_{soluble}) - 1$] is shown for the membrane-inserted toxin on native membranes (NM) vs. membranes containing the doxyl-stearic acid collisional quencher (NM + NO·).

inability of these toxins to insert their TMHs is responsible for loss of the cytolytic activity.

Because flow cytometry has not been previously used to measure membrane insertion of a transmembrane domain, we confirmed these results by using spectrofluorimetric methods to measure insertion of the TMHs into the bilayer of purified membranes from hRBCs (18). As can be seen in Fig. 5, the fluorescence intensity of the NBD probe in all three toxins increases significantly when the toxins are incubated with purified native erythrocyte ghost membranes (compare the fluorescence intensity of the soluble monomer to membrane-inserted oligomer on native membranes). Although the net increase for these toxins differed, the difference likely results primarily from differences in the starting environment of the probe in the soluble monomer (18, 29). NBD probes that occupy a more nonpolar site within the monomeric soluble protein will exhibit a smaller net increase in fluorescence intensity because they are moving from one nonpolar environment to another (i.e., the membrane core).

In agreement with the experiments shown in Fig. 4, the insertion of the TMHs did not occur on membranes derived from cholesterol-depleted hRBCs because the fluorescence intensity of the NBD probe remained the same as that of the soluble monomer in the absence of membranes (Fig. 5). On restoration of cholesterol to the cholesterol-depleted membranes, the intensity of the NBD increased to that observed when the toxins were incubated with native membranes, showing that only cholesterol was responsible for the loss of TMH insertion in the cholesterol-depleted membranes. We also examined the effect of adding cholesterol back to the membrane after the oligomeric complex of PFO had been preformed on cholesterol-depleted membranes. We found that the prepore could also efficiently insert under these conditions, indicating that the prepore oligomer that was formed on cholesterol-depleted membranes was still capable of insertion (data not shown).

The membrane location of the NBD-labeled residues was again confirmed for all three toxins by the accessibility of the NBD probe to collisional quenching by the membrane restricted 5- and 16-doxyl-stearic acid (Fig. 5). Although residue 215 of TMH1 of PFO has been rigorously demonstrated to enter the membrane (18) and has been used extensively to measure insertion of the PFO β-barrel (22, 24, 27, 29, 30), the equivalent residues of SLO and ILY have not. The NBD located at the equivalent positions in SLO and ILY also exhibits an increase in fluorescence intensity when incubated with membranes isolated from native hRBCs. Furthermore, the NBD located at these positions is collisionally quenched by the introduction of the 5- and 16-doxyl-stearic acid into those membranes (Fig. 5). Therefore, each of these residues faces the membrane bilayer and is a reliable indicator of TMH1 insertion by SLO and ILY.

Discussion

These studies show that the loss of prepore to pore conversion is the basis for the extreme sensitivity of CDC pore formation to the concentration of membrane cholesterol. Each primary independent step of the mechanism of CDC pore formation has been examined for its sensitivity to the depletion of membrane cholesterol from natural membranes. Furthermore, each stage of the cytolytic mechanism has been examined with three different CDC members to assess the generality of the cholesterol effect. In contrast to the long-held dogma that the primary effect of cholesterol depletion resides in the membrane-binding event, we have determined that the prepore to pore transition for each of these toxins is most sensitive to cholesterol depletion. Thus, the loss of cholesterol from the membrane abrogates cytolytic activity by preventing the membrane insertion of the transmembrane β-barrel of the prepore complex.

The results of the initial studies to examine the binding and cytolytic activity of PFO, SLO, and ILY on native and cholesterol-depleted hRBCs were unexpected. It was apparent that SLO and ILY erythrocyte binding was unaffected by the loss of 90% of the membrane cholesterol from the hRBCs, yet their cytolytic activity on the same cholesterol-depleted hRBCs was reduced >99.9%. Furthermore, even though the binding of PFO was reduced ≈10-fold on cholesterol depletion of the hRBCs, its activity was reduced >11,000-fold. Therefore, it was evident that the complete loss of cytolytic activity on the cholesterol-depleted hRBCs could not be reconciled by changes in the extent of membrane binding. Hence, the step in the cytolytic mechanism of the CDCs that was responsible for the hallmark sensitivity of these toxins to membrane cholesterol had to lie elsewhere in the mechanism.

When the oligomerization states of the bound CDCs were examined on native and cholesterol-depleted hRBCs, it was apparent that the depletion of membrane cholesterol did not significantly impact the conversion of bound monomer to oligomer although there seemed to be slightly less oligomer on the membrane of cholesterol-depleted hRBCs. Except in the case of PFO, this difference is probably due to the fact that the prepore oligomer of PFO is somewhat more sensitive to dissociation by SDS than is the pore complex (22, 27). The prepore is an oligomerized complex of the CDC monomers that has not yet inserted its transmembrane β-barrel and formed a pore. We have previously shown that the prepore complex is an essential intermediate in the pore-forming mechanism of these toxins (22, 24, 27, 28). PFO can be stalled or trapped in a prepore state by low temperature (24) or by various mutations within the PFO structure (22, 27). Likewise, cholesterol-depleted membranes trapped all three CDCs in the prepore state and prevented the insertion of the transmembrane β-barrel into the membrane and, therefore, pore formation. All three toxins regained full activity

if cholesterol was restored to the membrane, and so it is the loss of cholesterol alone that affects the prepore to pore conversion. These studies therefore show that the loss of cholesterol from the membrane traps PFO, as well as SLO and ILY, in their prepore complex and is primarily responsible for the hallmark sensitivity of the CDCs to membrane cholesterol.

Does cholesterol still function as the membrane receptor for these toxins? It is clear that PFO binding is reduced by depletion of membrane cholesterol although the extent of the reduction in binding was substantially less than the decrease in cytolytic activity. Thus, our data do not rule out an important role for cholesterol in the binding of some CDCs to the membrane, but it is clear that pore formation by PFO, SLO, and ILY is far more sensitive to cholesterol depletion of natural membranes than is their binding. This result was particularly evident for SLO and ILY because neither exhibited any significant change in binding on the cholesterol depleted membranes, yet both toxins were inactive on cholesterol-depleted cells. Therefore, although cholesterol may still function as a receptor for some or all CDCs at low concentrations, it is the loss of prepore to pore conversion that is most sensitive to membrane cholesterol levels.

The results of the present studies may also provide a paradigm for the general effect of cholesterol on the mechanism of widely divergent pore-forming toxins. Linder and Bernheimer (32) observed nearly two decades ago that the cytolytic activity of several pore-forming toxins was decreased by the depletion of membrane cholesterol. Since that time, the presence of membrane cholesterol has been found to enhance pore formation for the sea anenome-derived pore-forming toxin sticholysin II (33), *Staphylococcus aureus* alpha hemolysin (34), aerolysin (35), the earthworm-derived hemolysin eiseniapore (36), the *Escherichia coli* hemolysin ClyA (SheA) (37), and the *Vibrio cholerae* hemolysin (38). One explanation for the common enhancement of pore-formation is that cholesterol may interact with these toxins in such a way as to promote insertion of their transmembrane domains and/or by the promotion of certain membrane structures (inverted hexagonal phases) (39) that may facilitate the insertion of the transmembrane domains. Therefore, the enhancement in the conversion of pore-forming toxins to the membrane-inserted state may be a common effect of membrane cholesterol.

The studies herein show that the dominant effect of cholesterol on the CDC mechanism is to promote the insertion of the transmembrane β-barrel. These studies also provide a paradigm for the basis of cholesterol dependence for other pore-forming toxins whose mechanism is enhanced by the presence of membrane cholesterol.

The excellent technical help of Amy Marpoe is acknowledged. This work was supported by National Institutes of Health Grant AI37657 (to R.K.T.) and by the Robert A. Welch Foundation (A.E.J.).

1. Heuck, A. P., Tweten, R. K. & Johnson, A. E. (2001) *Biochemistry* **40,** 9065–9073.
2. Alouf, J. E. (1999) in *Bacterial Toxins: A Comprehensive Sourcebook*, eds. Alouf, J. & Freer, J. (Academic, London), pp. 443–456.
3. Alouf, J. E. (2000) *Int. J. Med. Microbiol.* **290,** 351–356.
4. Waheed, A. A., Shimada, Y., Heijnen, H. F., Nakamura, M., Inomata, M., Hayashi, M., Iwashita, S., Slot, J. W. & Ohno-Iwashita, Y. (2001) *Proc. Natl. Acad. Sci. USA* **98,** 4926–4931.
5. Jacobs, T., Cima-Cabal, M. D., Darji, A., Méndez, F. J., Vázquez, F., Jacobs, A. A. C., Shimada, Y., Ohno-Iwashita, Y., Weiss, S. & de los Toyos, J. R. (1999) *FEBS Lett.* **459,** 463–466.
6. Shimada, Y., Nakamura, M., Naito, Y., Nomura, K. & Ohno-Iwashita, Y. (1999) *J. Biol. Chem.* **274,** 18536–18542.
7. Nakamura, M., Sekino, N., Iwamoto, M. & Ohno-Iwashita, Y. (1995) *Biochemistry* **34,** 6513–6520.
8. Iwamoto, M., Nakamura, M., Mitsui, K., Ando, S. & Ohno-Iwashita, Y. (1993) *Biochim. Biophys. Acta* **1153,** 89–96.
9. Ohno-Iwashita, Y., Iwamoto, M., Mitsui, K., Ando, S. & Iwashita, S. (1991) *J. Biochem. (Tokyo)* **110,** 369–375.
10. Ohno-Iwashita, Y., Iwamoto, M., Ando, S., Mitsui, K. & Iwashita, S. (1990) *Biochim. Biophys. Acta* **1023,** 441–448.
11. Ohno-Iwashita, Y., Iwamoto, M., Mitsui, K., Ando, S. & Nagai, Y. (1988) *Eur. J. Biochem.* **176,** 95–101.
12. Shimada, Y., Maruya, M., Iwashita, S. & Ohno-Iwashita, Y. (2002) *Eur. J. Biochem.* **269,** 6195–6203.
13. Mobius, W., Ohno-Iwashita, Y., van Donselaar, E. G., Oorschot, V. M., Shimada, Y., Fujimoto, T., Heijnen, H. F., Geuze, H. J. & Slot, J. W. (2002) *J. Histochem. Cytochem.* **50,** 43–55.
14. Hagiwara, H., Kogure, S. Y., Nakamura, M., Shimada, Y., Ohno-Iwashita, Y. & Fujimoto, T. (1999) *Biochem. Biophys. Res. Commun.* **260,** 516–521.
15. Iwamoto, M., Morita, I., Fukuda, M., Murota, S., Ando, S. & Ohno-Iwashita, Y. (1997) *Biochim. Biophys. Acta* **1327,** 222–230.
16. Nagamune, H., Ohnishi, C., Katsuura, A., Fushitani, K., Whiley, R. A., Tsuji, A. & Matsuda, Y. (1996) *Infect. Immun.* **64,** 3093–3100.
17. Jacobs, T., Darji, A., Frahm, N., Rohde, M., Wehland, J., Chakraborty, T. & Weiss, S. (1998) *Mol. Microbiol.* **28,** 1081–1089.
18. Shepard, L. A., Heuck, A. P., Hamman, B. D., Rossjohn, J., Parker, M. W., Ryan, K. R., Johnson, A. E. & Tweten, R. K. (1998) *Biochemistry* **37,** 14563–14574.
19. Ho, S. N., Hunt, H. D., Horton, R. M., Pullen, J. K. & Pease, L. R. (1989) *Gene* **77,** 51–59.
20. Nelson, K. L. & Buckley, J. T. (2000) *J. Biol. Chem.* **275,** 19839–19843.
21. Klein, U., Gimpl, G. & Fahrenholz, F. (1995) *Biochemistry* **34,** 13784–13793.
22. Hotze, E. M., Wilson-Kubalek, E. M., Rossjohn, J., Parker, M. W., Johnson, A. E. & Tweten, R. K. (2001) *J. Biol. Chem.* **276,** 8261–8268.
23. Harris, R. W., Sims, P. J. & Tweten, R. K. (1991) *J. Biol. Chem.* **266,** 6936–6941.
24. Shepard, L. A., Shatursky, O., Johnson, A. E. & Tweten, R. K. (2000) *Biochemistry* **39,** 10284–10293.
25. Bradford, M. M. (1976) *Anal. Biochem.* **72,** 248–254.
26. Ilangumaran, S. & Hoessli, D. C. (1998) *Biochem. J.* **335,** 433–440.
27. Hotze, E. M., Heuck, A. P., Czajkowsky, D. M., Shao, Z., Johnson, A. E. & Tweten, R. K. (2002) *J. Biol. Chem.* **277,** 11597–11605.
28. Heuck, A. P., Tweten, R. K. & Johnson, A. E. (2003) *J. Biol. Chem.* **278,** 31218–31225.
29. Shatursky, O., Heuck, A. P., Shepard, L. A., Rossjohn, J., Parker, M. W., Johnson, A. E. & Tweten, R. K. (1999) *Cell* **99,** 293–299.
30. Heuck, A. P., Hotze, E., Tweten, R. K. & Johnson, A. E. (2000) *Mol. Cell* **6,** 1233–1242.
31. Bieri, V. G. & Wallach, D. F. (1975) *Biochim. Biophys. Acta* **406,** 415–423.
32. Linder, R. & Bernheimer, A. W. (1984) *Toxicon* **22,** 641–651.
33. de los Rios, V., Mancheno, J. M., Lanio, M. E., Onaderra, M. & Gavilanes, J. G. (1998) *Eur. J. Biochem.* **252,** 284–289.
34. Forti, S. & Menestrina, G. (1989) *Eur. J. Biochem.* **181,** 767–773.
35. Alonso, A., Goni, F. M. & Buckley, J. T. (2000) *Biochemistry* **39,** 14019–14024.
36. Lange, S., Nussler, F., Kauschke, E., Lutsch, G., Cooper, E. L. & Herrmann, A. (1997) *J. Biol. Chem.* **272,** 20884–20892.
37. Oscarsson, J., Mizunoe, Y., Li, L., Lai, X. H., Wieslander, A. & Uhlin, B. E. (1999) *Mol. Microbiol.* **32,** 1226–1238.
38. Zitzer, A., Zitzer, O., Bhakdi, S. & Palmer, M. (1999) *J. Biol. Chem.* **274,** 1375–1380.
39. Cheetham, J. J., Wachtel, E., Bach, D. & Epand, R. M. (1989) *Biochemistry* **28,** 8928–8934.